JOURNAL OF NANO- AND ELECTRONIC PHYSICS
Vol. **12** No 2, 02008(4pp) (2020)

ЖУРНАЛ НАНО- ТА ЕЛЕКТРОННОЇ ФІЗИКИ
Том **12** № 2, 02008(4cc) (2020)

Effect of Conductive Filament Temperature on ZrO_2 based Resistive Random Access Memory Devices

Pramod J. Patil[1,*], Namita A. Ahir[1], Suhas Yadav[1], Chetan C. Revadekar[1], Kishorkumar V. Khot[1], Rajanish K. Kamat[2], Tukaram D. Dongale[1], Deok-kee Kim[3,†]

[1] *Computational Electronics and Nanoscience Research Laboratory, School of Nanoscience and Biotechnology, Shivaji University, 416004 Kolhapur, India*
[2] *Department of Electronics, Shivaji University, 416004 Kolhapur, India*
[3] *Department of Electrical Engineering, Sejong University, 209 Neungdong-ro, Gwangjin-gu, 05006 Seoul, Republic of Korea*

(Received 16 February 2020; revised manuscript received 15 April 2020; published online 25 April 2020)

In the present work, the effect of reset voltage, filament radius, filament resistivity, and oxide membrane thickness on the nanoscale ZrO_2 RRAM devices was reported. The present investigation is based on the thermal reaction model of RRAM. The outcomes show a decline in saturated temperature with a rise in the radius and resistivity of filament. Furthermore, increases in saturated temperature with an increase in oxide membrane thickness were observed for the ZrO_2 based RRAM device. The saturated temperature of the device was mainly influenced by reset voltage, oxide layer thickness, filament size, and filament resistivity. The simulation results of the present investigation can be beneficial for the optimization of RRAM devices.

Keywords: Simulation, Resistive memory, Thermal reaction model, ZrO_2.

DOI: 10.21272/jnep.12(2).02008 PACS numbers: 78.20.Bh, 85.35. – p, 77.80.Fm.

1. INTRODUCTION

There is a huge demand for fast and scalable non-volatile memory devices for storing enormous data produced by the various information outbreaks. In view of this, the development of new memory material and devices is the need of the hour [1]. There are many potential candidates for the replacements for conventional silicon-based memory devices with enhanced scalability and performance. The resistive switching (RS) based non-volatile memory devices are among the best candidates to replace silicon-based memory devices [2]. Recent studies suggested that the resistive random access memory (RRAM) devices possess interesting properties required for data storage applications [3]. Among many materials, the ZrO2 is a probable candidate for the RRAM application. Awais et al. have used the electro-hydrodynamic printing method to fabricate the flexible ZrO2 resistive (memristive) a metal-insulator-metal switch. The developed device exhibited memristive characteristics in regular operation as well as after being physically stretched over 500 times [4]. Castán et al. have deposited ZrO_2:Al_2O_3 bilayer by the atomic layer deposition technique. They have studied the influence of dielectric composition and tested the devices for memory application. Their study suggested that the introduction of Al_2O_3 improves the RS properties of devices [5]. Chandrasekaran et al. have reported that switching characteristics of a ZrO_2-based electrochemical metallization memory examined by the effect of the TiW barrier layer [6]. Lee et al. have studied the effect of film thickness on ZrO_2 based ReRAM. Their study suggested that the memory window, retention and endurance properties can be improved by increasing the thickness of an active switching layer [7].

Along with experimental studies, various theoretical and simulation work for RS applications have been reported in the last few years [8-10]. The temperature is a noticeable parameter that affects the RS properties. Many efforts were carried out to study the effect of temperature on the RS. Recently, Witzleben et al. have observed the temperature effect on the switching kinetics of RS devices. Their study suggested that the heating of the device influences the switching speed [11]. Yi et al. have reported RS behaviors graphene oxide (GO) at different annealing temperatures. Their study suggested that the WORM type memory behaviors can be observed at lower annealing temperature and RS property declined with increases in annealing temperature [12]. Raffone et al. have examined the role of temperature in ReRAM switching by multiscale simulation. They have used kinetic Monte Carlo and finite difference methods and observed that the temperature is an essential factor in controlling the RS property [13].

Here, we have investigated the effect of the conductive filament temperature on ZrO_2 based RRAM devices using the thermal reaction model [14-15]. The temperature effect was studied by changing various physical parameters of the device such as oxide thickness, the radius of filament, resistivity of filament, and RESET voltage.

2. THERMAL REACTION MODEL

The thermal reaction model is centered around the forming and breaking of conductive filament localized within the oxide layer. It is interesting to know that the high current density $\sim 10^{-9}$ A/cm^2 is generally observed during the reset process. In view of this, the effect of temperature on the RS property is obvious.

---

[*] pramod.math@gmail.com.in
[†] deokkeekim@sejong.ac.kr

Therefore, it is important to investigate the temperature influence on RS properties. Fig. 1 represents a schematic of the thermal reaction model. The present model assumes a columnar filament path forming between two electrodes. Considering the resistance of filament (*R*) follows Ohms law, then the heating temperature ΔT is given as, [14].

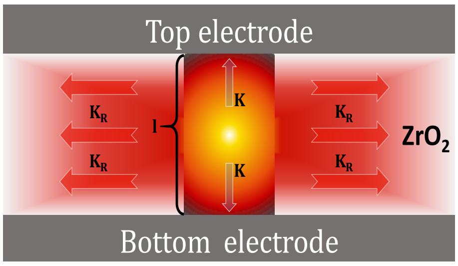

Fig. 1 – Cross-sectional view of the thermal reaction model used for simulation [14]

$$\Delta T = \frac{1}{\left(K_R + K\right)} \cdot \frac{V_{Reset}{}^2}{R}, \qquad (1)$$

where K is thermal conductance and K_R is radial thermal conductance, which is given as, [14]

$$K = \frac{k\pi r_1^2}{l/2} \qquad (2)$$

$$K_R = \frac{2\pi k' l/4}{\log\left(r_2/r_1\right)} \qquad (3)$$

where k and k' are thermal conductivities of materials, l is the oxide membrane thickness, r_1 is the conducting filament radius, and r_2 is a total radius [14].

$$r_2 = r_1 + \sqrt{\frac{4k'}{c'\gamma'}t} \qquad (4)$$

where C' and γ' specific heat and density of the material, and t is heating time. Table 1 represents the physical parameters for the simulation study.

Table 1 – Parameters varied during the simulation study

Reset voltage (V)	Oxide membrane thickness (nm)	Resistivity of filament (μΩ.cm)	Radius of filament (nm)
0.5	200	25	20
1.0	300	50	40
1.5	400	75	60
2.0	500	100	80
–	–	–	100

In the present analysis, we have studied the effect of the radius and resistivity of the filament with varying oxide membrane thickness and reset voltage on the saturation temperature behavior of the ZrO_2 RRAM device. Physical parameters used for simulation are as follows: thermal conductivity of ZrO_2 (k'): 0.035 W/cm/°C, thermal conductivity of Zr (k): 0.23 W/cm/°C, specific heat of ZrO_2 (C'): 0.475 J/g/°C and density of material (γ'): 5.9 g/cm^3.

3. RESULTS AND DISCUSSIONS

In the present study, we have used a ZrO_2 material as a case study owing to its remarkable RS and memory properties [16]. For the first case, we have studied the effect of oxide membrane thickness (varied from 200 nm to 500 nm) and the effect of filament resistivity (varied as 25, 50, 75, and 100 μΩ·cm) on the saturated temperature of filament at different VRESET (0.5, 1.0, 1.5, 2.0 V). Fig. 2 represents the exemplary results about the effect of resistivity and radius of the filament on the saturated temperature at 0.5 V reset voltage, 20 nm radius of the filament, 25 μΩ·cm resistivity of the filament and 200 nm oxide membrane thickness.

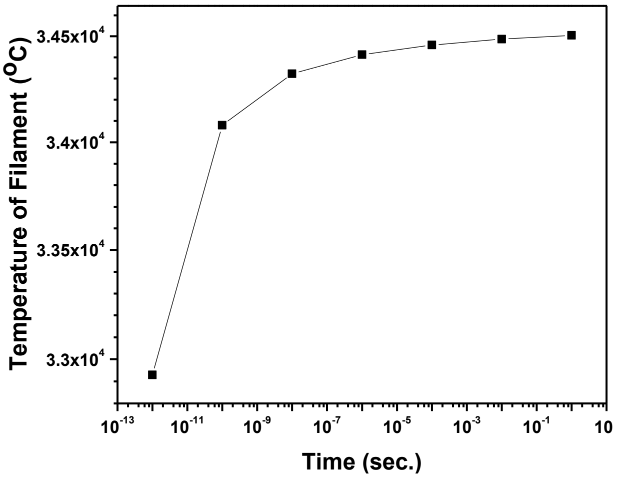

Fig. 2 – Exemplary results pertaining to the effect of resistivity and radius of the filament on the saturated temperature at 0.5 V reset voltage, 20 nm radius of the filament, 25 μΩ·cm resistivity of the filament and 200 nm oxide membrane thickness

Fig. 3 represents the effect of the above-mentioned parameters (Table 1) on the saturated temperature of the filament with respect to time. Fig. 2 shows the semi-log plot of the time domain saturation temperature effect. It is observed that the temperature increases gradually and gets saturated over a period of time. Furthermore, a sudden increase in the filament temperature is observed at the sub-nanosecond time scale, suggesting the complex RS dynamics play an important role. In Fig. 3a, the first line S1 represents 25 μΩ cm filament resistivity at 20 nm filament radius, S2 for 40 nm filament radius up to 100 nm (S5), S6 again for 50 μΩ cm with the same change in the oxide membrane thickness. For all other RESET voltages, the same pattern was observed, as shown in Fig. 3 (a to d).

For more convenience, the data of Fig. 3 are plotted on the double log scale. The saturated temperature values are summarized in Table 2. The results suggested that the minimum and maximum saturated temperature value increases as the RESET voltage varies from 0.5 V to 2.0 V. In addition to this, there is clear trend is observed for oxide thickness and saturated temperature values. It is observed that the minimum and maximum saturated temperature value increases as the active switching layer thickness varies between 200 nm to 500 nm.

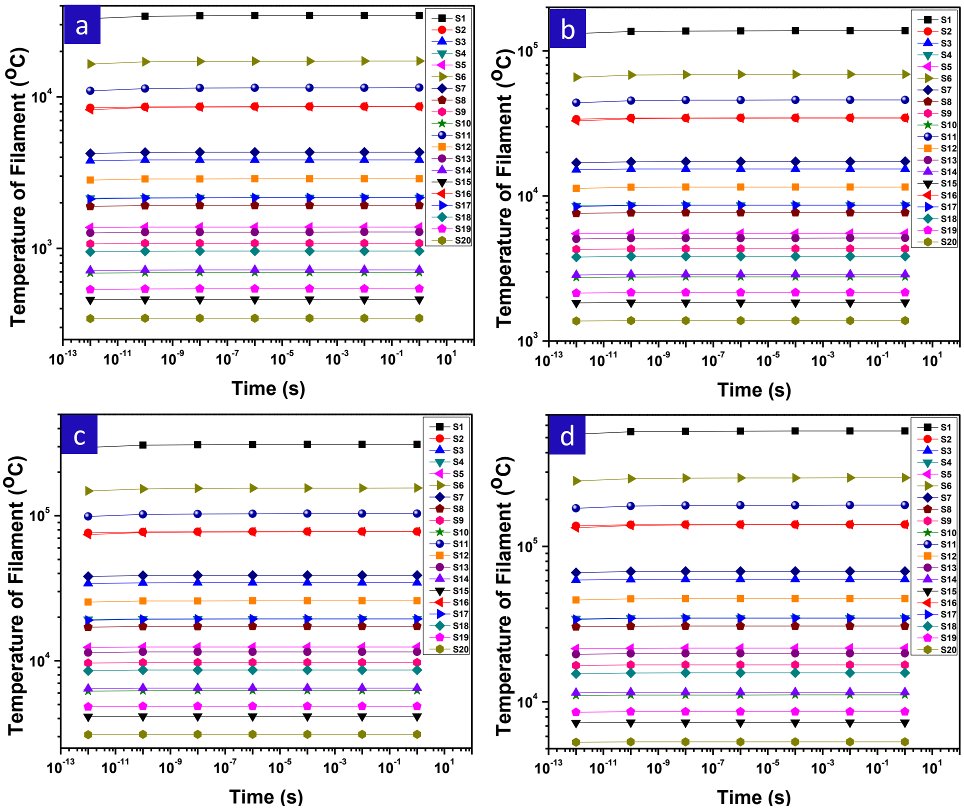

Fig. 3 – Effect of resistivity and radius of the filament on the saturated temperature at 0.5 (a), 1.0 (b), 1.5 (c), and 2.0 V (d) reset voltage with 200 nm oxide membrane thickness

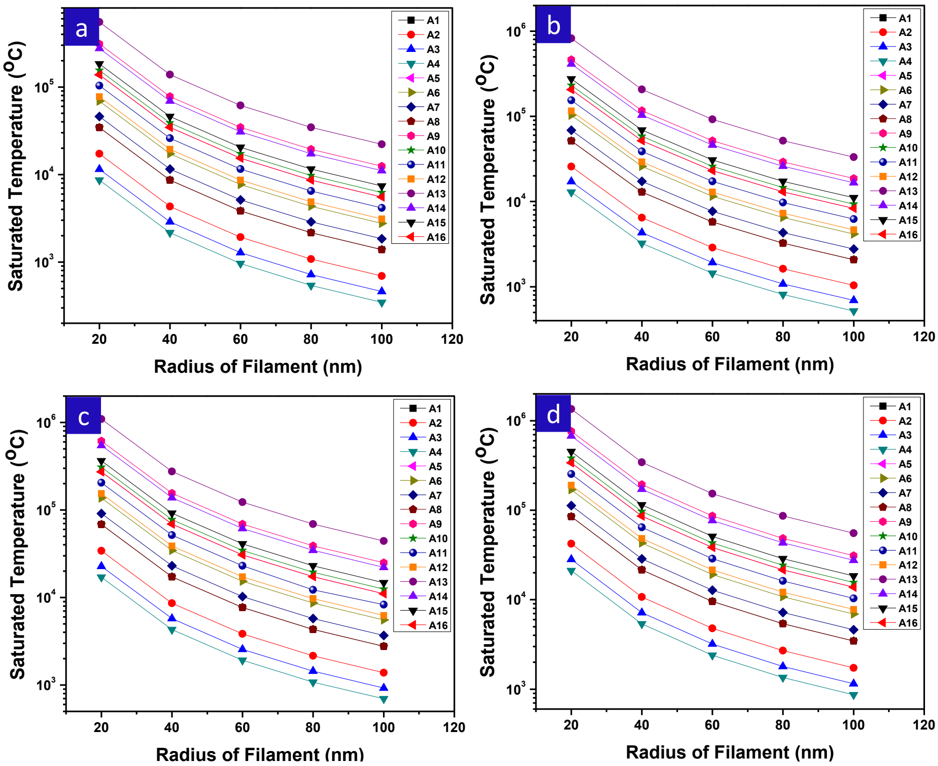

Fig. 4 – Effect of the radius of the filament on the saturated temperature at 0.5 (a), 1.0 (b), 1.5 (c), and 2.0 V (d) reset voltage with 200 nm oxide membrane thickness

Table 2 – Effect of the physical parameters on the saturated temperature

Oxide membrane thickness (nm)	V_Reset (V)	The maximum value of saturated temperature (°C)	The minimum value of saturated temperature (°C)
200	0.5	34504.64	343.40
	1.0	138018.58	1373.59
	1.5	310541.80	3090.59
	2.0	552074.30	5494.38
300	0.5	51581.31	510.32
	1.0	206325.26	2041.29
	1.5	464231.83	4592.89
	2.0	825301.04	8165.15
400	0.5	68449.86	671.71
	1.0	273799.45	2686.84
	1.5	616048.76	6045.38
	2.0	1095197.79	10747.35
500	0.5	85045.26	826.03
	1.0	340181.04	3304.11
	1.5	765407.34	7434.24
	2.0	1360724.16	13216.43

In addition to this, we have studied the effect of the radius of the filament on the saturation temperature, as shown in Fig. 4. The radius of the filament was varying between 20 nm to 100 nm. It is observed that the saturation temperature values decrease with the increase in the radius of the filament. The value for the 100 nm filament radius is nearly one-tenth than that of the value at 20 nm. This nature is observed for every change in resistivity of filament (from 25 μΩ.cm to 100 μΩ.cm). Furthermore, a clear trend of increasing the saturated temperature values with respect to increases in the RESET voltages are observed in the simulation results. In addition to this, this kind of nature is repeated for every oxide membrane thickness values, confirming that the increase in the radius of the filament led to a decrease in saturated temperature values.

4. CONCLUSIONS

The conductive filament temperature is an essential parameter of the RRAM devices and the saturated temperature is directly connected to the reliability of the memory devices. In general terms, the lower reliability of the device can be observed at a higher saturated temperature. In view of this, the small value of saturation temperature leads to high-performance RRAM devices. The results in the present investigation suggest that the temperature of the filament increases gradually and gets saturated over the period of time. Furthermore, a sudden increase in the filament temperature is observed at the sub-nanosecond time scale, suggesting the complex RS dynamics play an important role. The simulation results suggested that the minimum and maximum saturated temperature value increases as the RESET voltage varies from 0.5 V to 2.0 V and also increases as the active switching layer thickness varies from 200 nm to 500 nm. It is observed that the saturation temperature values decrease with the increase in the radius of the filament. Furthermore, a clear trend of increase in the saturated temperature values with respect to increases in the RESET voltages is observed. This kind of nature is repeated for every oxide membrane thickness values, confirming that the increase in the radius of the filament led to a decrease in saturated temperature values.

ACKNOWLEDGMENTS

Dr. P. J. Patil thank Shivaji University, Kolhapur for financial assistance under 'Research Initiation Scheme-2018'. This study was supported by the Basic research program (2016R1D1A1B01009537) through the National Research Foundation (NRF) of Korea and by the MOTIE (Ministry of Trade, Industry & Energy (10080581) and KSRC (Korea Semiconductor Research Consortium) support program for the development of the future semiconductor device.

REFERENCES

1. S. Balatti, S. Larentis, D.C. Gilmer, D. Ielmini, *Adv. Mater.* **25**, 1474 (2013).
2. R. Waser, R. Dittmann, G. Staikov, K. Szot, *Adv. Mater.* **21**, 2632 (2009).
3. J.J. Yang, D.B. Strukov, D.R. Stewart, *Nat. Nanotechnol.* **8**, 13 (2013).
4. M.N. Awais, H.C. Kim, Y.H. Doh, K.H. Choi, *Thin Solid Films* **536**, 308 (2013).
5. H. Castán, S. Dueñas, K. Kukli, M. Kemell, M. Ritala, M. Leskelä, *ECS Trans.* **85**, 143 (2018).
6. S. Chandrasekaran, F.M. Simanjuntak, T.Y. Tseng, *Jpn. J. Appl. Phys.* **57**, 04FE10 (2018).
7. S. Lee, T. Kim, B. Jang, W.Y. Lee, K.C. Song, H.S. Kim, G.Y. Do, S.B. Hwang, S. Chung, J. Jang, *IEEE Electron Device Lett.* **39**, 668 (2018).
8. S. Kim, S.J. Kim, K.M. Kim, S.R. Lee, M. Chang, E. Cho, Y.B. Kim, C.J. Kim, U.I. Chung, I.K. Yoo, *Sci. Rep.* **3**, 1680 (2013).
9. T.D. Dongale, K.P. Patil, S.B. Mullani, K.V. More, S.D. Delekar, P.S. Patil, P.K. Gaikwad, R.K. Kamat, *Sci. Semicond. Process.* **35**, 174 (2015).
10. T.D. Dongale, P.J. Patil, K.P. Patil, S.B. Mullani, K.V. More, S.D. Delekar, P.K. Gaikwad, R.K. Kamat, *J. Nano- Electron. Phys.* **7** No 3, 03012 (2015).
11. M. von Witzleben, K. Fleck, C. Funck, B. Baumkötter, M. Zuric, A. Idt, T. Breuer, R. Waser, U. Böttger, S. Menzel, *Adv. Electron. Mater.* **3**, 1700294 (2017).
12. M. Yi, Y. Cao, H. Ling, Z. Du, L. Wang, T. Yang, Q. Fan, L. Xie, W. Huang, *Nanotechnol.* **25**, 185202 (2014).
13. F. Raffone, G. Cicero, *ACS Appl. Mater. Interface.* **10**, 7512 (2018).
14. Y. Sato, K. Kinoshita, M. Aoki, Y. Sugiyama, *Appl. Phys. Lett.* **90**, 033503 (2007).
15. T.D. Dongale, K.V. Khot, S.V. Mohite, S.S. Khandagale, S.S. Shinde, V.L. Patil, S.A. Vanalkar, A.V. Moholkar, K.Y. Rajpure, P.N. Bhosale, P.S. Patil, *J. Nano- Electron. Phys.* **8** No 4, 04030 (2016).
16. X. Wu, P. Zhou, J. Li, L.Y. Chen, H.B. Lv, Y.Y. Lin, T.A. Tang, *Appl. Phys. Lett.* **90**, 183507 (2007).